ORIGINAL ARTICLE

Synthesis and Surface Properties of *N,N*-Dimethyl-*N*-dodecyl Polyoxyethylene Amine-Based Surfactants: Amine Oxide, Betaine and Sulfobetaine

**Liya Hou · Huinian Zhang · Hui Chen · Qibo Xia ·
Dongyang Huang · Li Meng · Xuefeng Liu**

Abstract Nonionic–zwitterionic hybrid surfactants, namely *N,N*-dimethyl-*N*-dodecyl polyoxyethylene (3) amine oxide, and the corresponding betaine and/or sulfobetaine, have been synthesized. Their molecule structures were characterized by means of electrospray ionization mass spectrometry and ^{1}H nuclear magnetic resonance. Compared to the structurally related conventional amine oxide, betaine and sulfobetaine, the critical micelle concentrations of the three hybrid surfactants are one order of magnitude smaller than those of traditional ones. The polyoxyethylene segment between the hydrophilic head group and the hydrophobic tail makes the surface activities of the hybrid surfactants superior to their structure-related counterparts.

Keywords Hybrid surfactant · *N,N*-Dimethyl-*N*-dodecyl polyoxyethylene (3) amine · Amine oxide · Betaine · Sulfobetaine
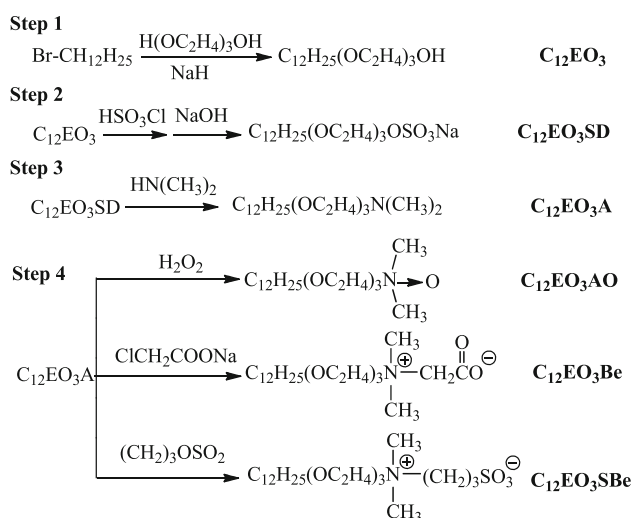
Introduction

Ethoxylated surfactants, especially those having a chain segment of polyoxyethylene between hydrophilic head group and hydrophobic tail, are called hybrid surfactants [1, 2]. The traditional representatives are alcohol ether sulfates (AES) [3, 4], alcohol ether carboxylates (AEC) [5] and sodium alkyl-benzyl polyoxyethylenated propane sulfonates (ABEPS) [2]. These nonionic–ionic hybrid surfactants always present combined properties of nonionic and ionic surfactants [2] and have better electrolyte and water hardness tolerance. However, the literature reports on hybrid surfactants are mainly on nonionic–anionic surfactants, the synthesis and the surface activity of nonionic–zwitterionic hybrid surfactants have seldom been reported up till now.

One US patent [6] reveals the synthesis of *N,N*-dimethyl-*N*-alkyl polyoxyethylene amine and the corresponding amine oxides from commercial available AES. One Japanese patent [7] reveals the synthesis of *N,N*-dimethyl-*N*-alkyl polyoxyethylene amine-based betaines from commercial available fatty alcohols. However, the typical physicochemical properties of these hybrid surfactants, such as the critical micelle concentration (CMC), the surface tension at CMC (γ_{CMC}), the adsorption efficiency (pC_{20}), the surface pressure at the CMC (Π_{CMC}), the maximum surface excess (Γ_m), the minimum cross-sectional area (A_{min}) have not been reported. Due to the length distribution of the alkyl tail and the polyoxyethylene segment in commercially available AES and polyethoxylated fatty alcohols, the corresponding amine oxides and betaines are mixtures of different molecules. In order to get the typical surface activity parameters of nonionic–zwitterionic hybrid surfactants and to compare them with structure-related traditional ones, three hybrid surfactants,

L. Hou · H. Zhang · H. Chen · Q. Xia · D. Huang · L. Meng
School of Chemical and Material Engineering,
Jiangnan University, Wuxi 214122, China

X. Liu (✉)
The Key Laboratory of Food Colloids and Biotechnology,
Ministry of Education, School of Chemical and Material
Engineering, Jiangnan University, Wuxi 214122, China
e-mail: xfliu@jiangnan.edu.cn

Step 1

$$Br\text{-}CH_{12}H_{25} \xrightarrow[\text{NaH}]{H(OC_2H_4)_3OH} C_{12}H_{25}(OC_2H_4)_3OH \qquad \mathbf{C_{12}EO_3}$$

Step 2

$$C_{12}EO_3 \xrightarrow[\text{}]{HSO_3Cl \;\; NaOH} C_{12}H_{25}(OC_2H_4)_3OSO_3Na \qquad \mathbf{C_{12}EO_3SD}$$

Step 3

$$C_{12}EO_3SD \xrightarrow{HN(CH_3)_2} C_{12}H_{25}(OC_2H_4)_3N(CH_3)_2 \qquad \mathbf{C_{12}EO_3A}$$

Step 4

$$\xrightarrow{H_2O_2} C_{12}H_{25}(OC_2H_4)_3\overset{CH_3}{\underset{CH_3}{N}}\rightarrow O \qquad \mathbf{C_{12}EO_3AO}$$

$$C_{12}EO_3A \xrightarrow{ClCH_2COONa} C_{12}H_{25}(OC_2H_4)_3\overset{CH_3}{\underset{CH_3}{\overset{\oplus}{N}}}\text{—}CH_2\overset{O}{\overset{\|}{C}}O^{\ominus} \qquad \mathbf{C_{12}EO_3Be}$$

$$\xrightarrow{(CH_2)_3OSO_2} C_{12}H_{25}(OC_2H_4)_3\overset{CH_3}{\underset{CH_3}{\overset{\oplus}{N}}}\text{—}(CH_2)_3SO_3^{\ominus} \qquad \mathbf{C_{12}EO_3SBe}$$

Scheme 1 The synthesis routes of $C_{12}EO_3AO$, $C_{12}EO_3Be$ and $C_{12}EO_3SBe$

namely *N,N*-dimethyl-*N*-dodecyl polyoxyethylene (3) amine-based amine oxide ($C_{12}EO_3AO$), and the corresponding betaine ($C_{12}EO_3Be$) and sulfobetaine ($C_{12}EO_3SBe$) were synthesized (see Scheme 1). The molecular structures of the main intermediates and objective surfactants were confirmed by means of electrospray ionization mass spectrometry (ESI–MS), and ^1H nuclear magnetic resonance (^1H NMR), respectively. The typical physicochemical properties of CMC, γ_{CMC}, pC_{20}, Γ_m, and A_{min} were determined and calculated from the results of γ-$\log c$ (concentration of surfactant) curves.

Experimental Section

Materials

1-Bromododecane (Br-C_{12}), triethylene glycol (EO_3), sodium hydride (NaH), dimethylamine (DMA), sodium chloroacetate, 1,3-propanesultone and H_2O_2 (30 wt%) were used as received without further purification. Deionized water was obtained from a Millipore Milli-Q water purification system (Millipore, USA).

Synthesis of $C_{12}EO_3$

As shown in Scheme 1 (Step 1), NaH (4.80 g) and EO_3 (72.08 g) were added to a 250-mL three-neck round-bottom flask. Br-C_{12} (26.54 g) was added drop wise to the flask with stirring at 100 °C. The reaction was protected by N_2 and completed in 48 h. Then, 80 mL ethyl acetate was added to the flask. The excess EO_3 and the by-product polyethylene glycol were washed off using saturated NaCl aqueous solution. The faint yellow crude product was

obtained after the solvent was removed by rotary evaporator under reduced pressure. Finally, the crude $C_{12}EO_3$ was purified by silica gel column chromatography. A mixture of mineral ether–ethyl acetate (volume ratio 2:1) was used as the eluent. A colorless liquid of $C_{12}EO_3$ was obtained with a yield of 61 %.

Synthesis of $C_{12}EO_3A$

HSO_3Cl (12.82 g) was added dropwise to $C_{12}EO_3$ (31.8 g) at 25–30 °C, after that, the system was aged for 0.5 h. After being neutralized by 15 % NaOH aqueous solution, the product of $C_{12}EO_3SD$ (Scheme 1, Step 2) was obtained. According to the method in [6, 8], a light yellow oil liquid of $C_{12}EO_3A$ (Scheme 1, Step 3) was synthesized with a yield of 94 %.

Synthesis of $C_{12}EO_3AO$

As shown in Scheme 1 (Step 4), $C_{12}EO_3A$ (34.51 g) was oxidized by 30 % H_2O_2 (45.37 g, dropwise) at 55–65 °C with a trace amount of citric acid. The crude $C_{12}EO_3AO$ was extracted by $CHCl_3$ and was purified by alumina column chromatography. A mixture of $CHCl_3$–CH_3OH (volume ratio 60:1) was used as the eluent. $C_{12}EO_3AO$ was obtained with a yield of 91 %.

Synthesis of $C_{12}EO_3Be$

In a 250-mL round-bottom flask, $C_{12}EO_3A$ (17.31 g) and sodium chloroacetate (5.83 g) were dissolved in 100 mL methanol–H_2O (volume ratio 1:1), the pH of the above system was adjusted to 7–8 by $NaHCO_3$. The reaction was carried out at 70 °C for 2 h, then 80 °C for a further 2 h. The solvent was removed by rotary evaporation under reduced pressure. The residue was dried in a vacuum oven at 70 °C. The dried residue was dissolved in isopropanol, and inorganic salts were filtered off. The crude $C_{12}EO_3Be$ was purified by silica gel column chromatography. A mixture of ethyl acetate–CH_3OH (volume ratio 3:1) was used as the eluent. $C_{12}EO_3Be$ was obtained with a yield of 89 %.

Synthesis of $C_{12}EO_3SBe$

In a 250-mL round-bottom flask, $C_{12}EO_3A$ (17.31 g) was dissolved in 80 mL acetone in an ice-water bath, then 6.72 g 1,3-propanesultone in 80 mL acetone was added dropwise to the flask with stirring. After the addition of 1,3-propanesultone, the temperature of the system was elevated to room temperature naturally. The reaction was carried out for 5 days at room temperature with stirring. The white crude $C_{12}EO_3SBe$ was purified by silica gel column chromatography. A mixture of $CHCl_3$–CH_3OH
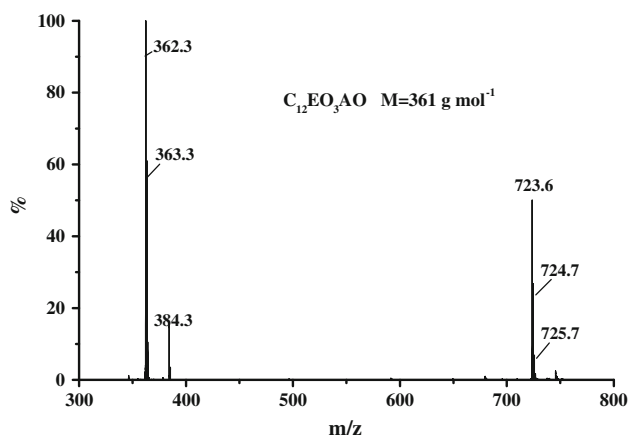
Fig. 1 The ESI–MS spectrum of $C_{12}EO_3AO$ with positive ion mode
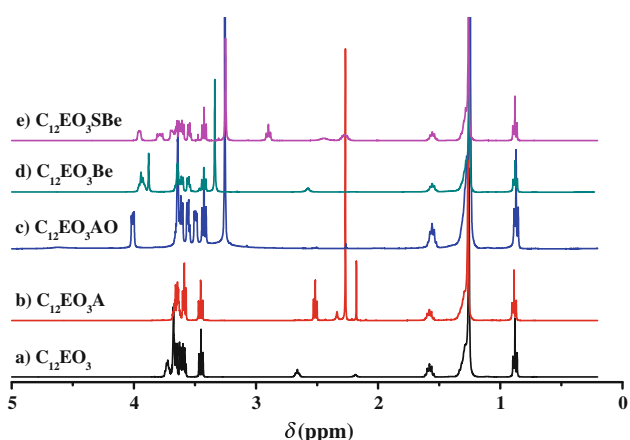

Fig. 2 The ^1H NMR spectrum of a $C_{12}EO_3$, b $C_{12}EO_3A$, c $C_{12}EO_3AO$, d $C_{12}EO_3Be$ and e $C_{12}EO_3SBe$

Fig. 3 The plot of surface tension (γ in mN m^{-1}) versus drop surface aging time (t in min) for $C_{12}EO_3AO$ and $C_{12}EO_3Be$ aqueous solution at 25 °C, the concentration of the surfactant was 3.0×10^{-5} mol L^{-1}

(volume ratio 4:1) was used as the eluent. $C_{12}EO_3SBe$ was obtained with a yield of 76 %.

Analytical Methods

The ESI–MS measurements were carried out using a Maldi Synapt Q-TOF MS (Waters) in the positive ion mode (Fig. 1, ESM Figure 1S). The ^1H NMR spectra were obtained with an Avance III 400 MHz digital NMR spectrometer (Bruker) using CDCl$_3$ as solvent (Fig. 2). And the NMR peak of CDCl$_3$ ($\delta = 7.26$ ppm) was used as the reference in determining the chemical shifts (δ, ppm) of the protons.

The surface tension (γ, mN m^{-1}) measurements were conducted with a drop volume tensiometer at 25 ± 0.1 °C. The outer radius of the glass capillary was 0.66 mm. During the procedure of γ measurements, a sufficient aging time was necessary for the pendant drop surface to reach an equilibrium state. The aging time of the drop surface was determined by the plot of γ versus the drop detachment
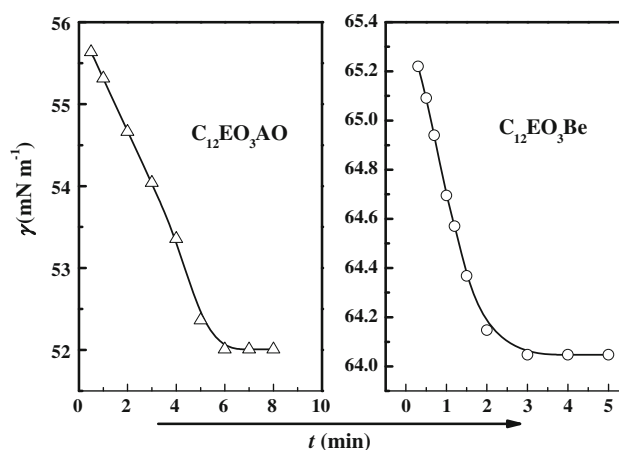
time t (min) (Fig. 3). Finally, the drop volume was corrected by the Harkins–Brown method [9]. The surface activity parameters, such as the CMC, the γ at CMC (γ_{CMC}), the adsorption efficiency (pC_{20}), the surface pressure at the CMC (Π_{CMC}), the maximum surface excess (Γ_m), and the minimum cross-sectional area (A_{min}) were obtained or calculated [10] from the γ-log$c$ curves (Fig. 4).

Results and Discussion

Structural Characterization of $C_{12}EO_3$, $C_{12}EO_3A$, $C_{12}EO_3AO$, $C_{12}EO_3Be$ and $C_{12}EO_3SBe$

The ESI–MS technique was employed to measure the molecule weight of the products in this work. The ESI–MS spectrum of $C_{12}EO_3AO$ is shown in Fig. 1. With the positive ion mode, various ions of [M+H]$^+$, [M+Na]$^+$ and [2M+H]$^+$ were detected. The ESI–MS spectra of the rest samples (surfactants of $C_{12}EO_3Be$ and $C_{12}EO_3SBe$, intermediates of $C_{12}EO_3$ and $C_{12}EO_3A$) can be seen in Figure 1S as ESM. The results obtained of the mass-to-charge ratio (m/z) for the three hybrid surfactants match well with the calculated results. The interpretation of the ESI–MS spectra can be seen in detail in the ESM.

In order to obtain the detailed molecule structural information, the ^1H NMR spectra of the objective compound were obtained (Fig. 2). $C_{12}EO_3$ ^1H NMR [400 MHz, (CDCl$_3$)] $\delta = 0.86$–0.90 (t, 3H, –CH_3), $\delta = 1.26$–1.29 (m, 18H, –(CH_2)$_9$–), $\delta = 1.54$–1.61 (m, 2H, C$_{10}$–CH_2–CH$_2$–O), $\delta = 2.66$ (s, 1H, –OH), $\delta = 3.43$–3.47 (t, 2H, C$_{10}$–CH$_2$–CH_2–O), $\delta = 3.58$–3.74 (m, 12H, C$_{12}$–(OC$_2$$H_4$)$_3$–). $C_{12}EO_3A$ ^1H NMR [400 MHz, (CDCl$_3$)] $\delta = 0.86$–0.90 (t, 3H, –CH_3), $\delta = 1.26$–1.29 (m, 18H, –(CH_2)$_9$–),
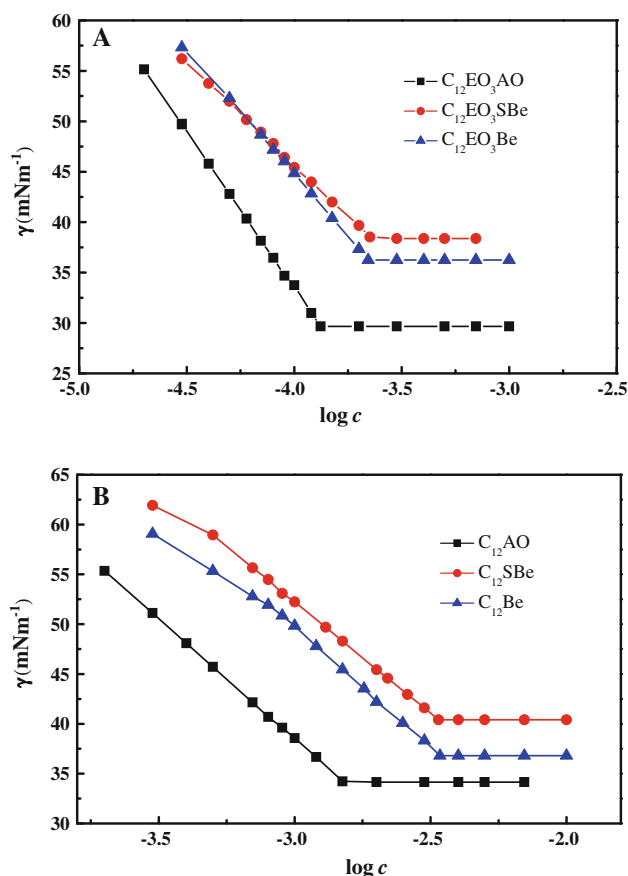
Fig. 4 The plots of the surface tension (γ in mN m^{-1}) versus $\log c$ (concentration of surfactant in mol L^{-1}) at 25 °C

$\delta = 1.56$–1.59 (m, 2H, C$_{10}$–C$\boldsymbol{H}_2$–CH$_2$–O), $\delta = 2.26$ (s, 6H, N–(C$\boldsymbol{H}_3$)$_2$), $\delta = 2.49$–2.52 (t, 2H, –C$\boldsymbol{H}_2$–N), $\delta = 3.43$–3.46 (t, 2H, C$_{11}$–C$\boldsymbol{H}_2$ –O), $\delta = 3.57$–3.66 (m, 10H, C$_{12}$–(OC$_2\boldsymbol{H}_4$)$_2$–OC$\boldsymbol{H}_2$–). **C$_{12}$EO$_3$AO** ^{1}H NMR [400 MHz, (CDCl$_3$)] $\delta = 0.86$–0.90 (t, 3H, –C$\boldsymbol{H}_3$), $\delta = 1.26$–1.29 (m, 18H, –(C$\boldsymbol{H}_2$)$_9$–), $\delta = 1.55$–1.59 (m, 2H, C$_{10}$–C$\boldsymbol{H}_2$–CH$_2$–O), $\delta = 3.25$ (s, 6H, N–(C$\boldsymbol{H}_3$)$_2$), $\delta = 3.40$–3.44 (t, 2H, C$_{11}$–C$\boldsymbol{H}_2$–O), $\delta = 3.48$–3.52 (t, 2H, –C$\boldsymbol{H}_2$–N), $\delta = 3.55$–3.65 (m, 8H, C$_{12}$–(OC$_2\boldsymbol{H}_4$)$_2$–O), $\delta = 4.00$ (t, 2H, –O–C$\boldsymbol{H}_2$CH$_2$N). **C$_{12}$EO$_3$Be** ^{1}H NMR [400 MHz, (CDCl$_3$)] $\delta = 0.86$–0.89 (t, 3H, –C$\boldsymbol{H}_3$), $\delta = 1.26$ (m, 18H, –(C$\boldsymbol{H}_2$)$_9$–), $\delta = 1.52$–1.57 (m, 2H,

C$_{10}$H$_{21}$–C$\boldsymbol{H}_2$–CH$_2$–O), $\delta = 3.34$ (s, 6H, N–(C$\boldsymbol{H}_3$)$_2$), $\delta = 3.41$–3.44 (t, 2H, –C$\boldsymbol{H}_2$–N), $\delta = 3.55$–3.56 (t, 2H, C$_{11}$–C$\boldsymbol{H}_2$–O), $\delta = 3.60$–3.61 (t, 2H, O–C$\boldsymbol{H}_2$–CH$_2$N), $\delta = 3.62$–3.65 (m, 4H, C$_{12}$–O–C$_2\boldsymbol{H}_4$–O), $\delta = 3.88$ (s, 2H, N–C$\boldsymbol{H}_2$COO), $\delta = 3.93$–3.96 (m, 4H, O–C$_2\boldsymbol{H}_4$–OC$_2$H$_4$N). **C$_{12}$EO$_3$SBe** ^{1}H NMR [400 MHz, (CDCl$_3$)] $\delta = 0.86$–0.90 (t, 3H, –C$\boldsymbol{H}_3$), $\delta = 1.29$ (m, 18H, –(C$\boldsymbol{H}_2$)$_9$–), $\delta = 1.52$–1.57 (m, 2H, C$_{10}$H$_{21}$–C$\boldsymbol{H}_2$–CH$_2$–O), $\delta = 2.27$ (m, 2H, –CH$_2$–C$\boldsymbol{H}_2$–CH$_2$–S), $\delta = 2.90$ (t, 2H, –C$\boldsymbol{H}_2$–CH$_2$–CH$_2$–S), $\delta = 3.28$ (s, 6H, N–(C$\boldsymbol{H}_3$)$_2$), $\delta = 3.43$–3.45 (t, 2H, –C$\boldsymbol{H}_2$–N), $\delta = 3.50$–3.55 (t, 2H, C$_{11}$–C$\boldsymbol{H}_2$–O), $\delta = 3.57$–3.67 (m, 8H, C$_{12}$H$_{25}$–(OC$_2\boldsymbol{H}_4$)$_2$–O), $\delta = 3.79$ (t, 2H, O–C$\boldsymbol{H}_2$–CH$_2$N), $\delta = 3.95$ (t, 2H, –C$\boldsymbol{H}_2$–S).

The Surface Activity Parameters of C$_{12}$EO$_3$AO, C$_{12}$EO$_3$Be and C$_{12}$EO$_3$SBe

As shown in Fig. 3, the γ of the solution (3.0×10^{-5} mol L^{-1}) decreases with the drop detachment time increasing with breakpoints at $t \approx 3$ min (for C$_{12}$EO$_3$Be) and $t \approx 6$ min (for C$_{12}$EO$_3$AO), respectively. The result of C$_{12}$EO$_3$SBe is similar to that of C$_{12}$EO$_3$Be. The change of γ is $<\pm 0.1$ mN m^{-1} in the region of $t > 10$ min. Under this condition, the γ could be considered as an equilibrium surface tension. The lower concentration sample solution needs longer aging time for the drop surface to reach the equilibrium state. Thus, in order to make the drop surfaces reach the equilibrium state, all the drops of the surfactant solutions were aged for at least 10 min.

The plots of the γ versus $\log c$ for the hybrid surfactants in this work and the corresponding traditional surfactants are shown in Fig. 4. One can see that the γ gradually decreases to a plateau region with the surfactant concentration increasing. A decrease in surface tension indicates that the surfactant molecules adsorbed at the air-solution interfaces. The break point appearing in the γ-$\log c$ curves suggests the formation of micelles in aqueous solutions. Here, it is worth mentioning that no evidence of surface tension minima appears in the γ-$\log c$ curves [11]. The surface activity parameters, such as CMC, γ_{CMC}, pC_{20}, Π_{CMC}, Γ_m and A_{min} were obtained and/or calculated [10] from the γ-$\log c$ curves and are listed in Table 1.

Table 1 The calculated parameters of surfactants from γ-$\log c$ curves at 25 °C

	C$_{12}$EO$_3$AO	C$_{12}$AO	C$_{12}$EO$_3$Be	C$_{12}$Be	C$_{12}$EO$_3$SBe	C$_{12}$SBe
CMC (mol L^{-1})	1.32×10^{-4}	1.53×10^{-3}	2.30×10^{-4}	3.42×10^{-3}	2.25×10^{-4}	3.38×10^{-3}
γ_{CMC} (mN m^{-1})	29.66	34.15	36.24	36.79	38.39	40.40
Π_{CMC} (mN m^{-1})	42.36	37.87	35.78	35.23	33.63	31.62
pC_{20}	4.52	3.55	4.28	3.09	4.29	2.99
Γ_m (mol cm^{-2})	5.02×10^{-6}	4.71×10^{-6}	4.74×10^{-6}	4.52×10^{-6}	3.82×10^{-6}	4.49×10^{-6}
A_{min} (m^2)	3.31×10^{-19}	3.53×10^{-19}	3.50×10^{-19}	3.68×10^{-19}	4.35×10^{-19}	3.70×10^{-19}

The CMC for *N,N*-dimethyl-*N*-dodecyl amine oxide (C$_{12}$AO) is 1.18×10^{-3} mol L^{-1} (ring method) [12], for *N,N*-dimethyl-*N*-dodecyl betaine (C$_{12}$Be) 2.00×10^{-3} mol L^{-1} (ring method) [13], and for *N,N*-dimethyl-*N*-dodecyl sulfobetaine (C$_{12}$SBe) is 2.20×10^{-3} mol L^{-1} (maximum bubble pressure method) [14], respectively. As can be seen in Table 1, the CMC values of C$_{12}$AO, C$_{12}$Be and C$_{12}$SBe in this work match well with those in the literature [12–14] despite the difference in the γ determination methods. All the CMC values of the hybrid surfactants in this work fall within the 10^{-4} mol L^{-1} range, which is one order of magnitude smaller than those of structure related traditional surfactants. The similar relations hold true for sodium dodecyl sulfate and dodecyl polyoxyethylene sulfates [2, 15]. It could be attributed to the hydrophilicity of the hybrid surfactants in this work 'continuously' increasing from hydrophobic (C$_{12}$) to less hydrophobic/less hydrophilic (EO$_3$) then to hydrophilic (AO, Be, and SBe). As regards the change in the hydrophilicity at the water–air interface, one can argue that it changes from hydrophobic (air) over a less hydrophobic/less hydrophilic interfacial zone (EO$_3$) between the two bulk phases to hydrophilic (water) [1]. However, the hydrophilicity of the structure-related counterparts changes 'discontinuously' from hydrophobic tails to hydrophilic head groups without a less hydrophobic/less hydrophilic transition zone (EO$_3$), which, in turn, explains the higher surface activity of the hybrid surfactants in this work.

If one looks at the structure difference among the hybrid surfactants in this work, one sees the main structure difference lies in the head groups of AO, Be and SBe. Due to AO being a totally non-ionic head group, it has the smallest hydrophilicity among these three head groups. Be and SBe are zwitterionic head groups, possessing higher hydrophilicity than that of AO. However, the head group of Be is more hydrophilic than the SBe ones [14]. The hydrophilic difference of the head groups leads to the difference in the CMC values. The order of the CMC values for the hybrid surfactants in this work is CMC$_{AO}$ < CMC$_{SBe}$ < CMC$_{Be}$, a similar relation can be observed in structure related unethoxylated ones. It could be attributed to the hydrophilic difference of the head groups [14].

References

1. Catanoiu G, Blunk D, Stubenrauch C (2012) Novel ethoxylated inositol derivatives—hybrid carbohydrate/oligoethylene oxide surfactants. J Colloid Interface Sci 371:82–88
2. Wang X, Yan F, Li Z, Zhang L, Zhao S, An J, Yu J (2007) Synthesis and surface properties of several nonionic–anionic surfactants with straight chain alkyl-benzyl hydrophobic group. Colloids Surf A 302:532–539
3. Tokiwa F, Ohki K (1967) Micellar properties of a series of sodium dodecylpolyoxyethylene sulfates from hydrodynamic data. J Phys Chem 71(5):1343–1348
4. Alargova RG, Ivanova VP, Kralchevsky PA, Mehreteab A, Broze G (1998) Growth of rod-like micelles in anionic surfactant solutions in the presence of Ca^{2+} counterions. Colloids Surf A 142:201–218
5. Gong R, Han L, Gao C, Shu M, Che S (2009) Molecular design of AEC tri-block anionic surfactant towards rational synthesis of targeted thick-walled mesoporous silica. J Mater Chem 19:3404–3411
6. Koebner A, Potts HA (1965) *N*-dialkyl-alkyl- and alkaryl-oxy-alkyl-amine oxides. US Patent 3,206,512
7. Yoshinobu N (1985) Ampholytic surface-active betaine compound and production thereof. J.P. Patent 60,089,458
8. Lange F, Meffert A (1987) Process for preparing tertiary ether amines. US 4,650,865
9. Harkins WD, Brown F (1919) The determination of surface tension (free surface energy), and the weight of falling drops: the surface tension of water and benzene by the capillary height method. J Am Chem Soc 41:499–524
10. Liu XF, Hu J, Huang YJ, Fang Y (2013) Aggregation behavior of surface active dialkylimidazolium ionic liquids [C$_{12}$C$_{nim}$]Br ($n = 1$–4) in aqueous solutions. J Surfactants Deterg 16:539–546
11. Mohamed A, Trickett K, Chin SY, Cummings S, Sagisaka M, Hudson L, Nave S, Dyer R, Rogers SE, Heenan RK, Eastoe J (2010) Universal surfactant for water, oils, and CO$_2$. Langmuir 26:13861–13866
12. Goracci L, Germani R, Rathman JF, Savelli G (2007) Anomalous behavior of amine oxide surfactants at the air/water interface. Langmuir 23:10525–10532
13. Chevalier Y, Storet Y, Pourchet S, Perchec PL (1991) Tensioactive properties of zwitterionic carboxybetaine amphiphiles. Langmuir 7:848–853
14. Weers JG, Rathman JF, Axe FU, Crichlow CA, Foland LD, Scheuing DR, Wiersema RJ, Zielske AG (1991) Effect of the intramolecular charge separation distance on the solution properties of betaines and sulfobetaines. Langmuir 7:854–867
15. Rosen MJ (2004) Surfactants and interfacial phenomena, 3rd edn. Wiley, New Jersey, pp 129–135

Author Biographies

Liya Hou is a graduate student, majoring in applied chemistry at the School of Chemical and Material Engineering, Jiangnan University, Wuxi, People's Republic of China.

Huinian Zhang is a graduate student, majoring in applied chemistry at the School of Chemical and Material Engineering, Jiangnan University, Wuxi, People's Republic of China.

Hui Chen is a graduate student, majoring in applied chemistry at the School of Chemical and Material Engineering, Jiangnan University, Wuxi, People's Republic of China.

Qibo Xia is a graduate student, majoring in applied chemistry at the School of Chemical and Material Engineering, Jiangnan University, Wuxi, People's Republic of China.

Dongyang Huang is a undergraduate student, majoring in applied chemistry in the School of Chemical and Material Engineering, Jiangnan University, Wuxi, People's Republic of China.

Li Meng is a undergraduate student, majoring in applied chemistry in the School of Chemical and Material Engineering, Jiangnan University, Wuxi, People's Republic of China.

Xuefeng Liu received his M.Sc. degree from Wuxi University of Light Industry, and his Ph.D. from Jiangnan University in China. He is a professor at the Key Laboratory of Food Colloids and Biotechnology, Ministry of Education, and the Chairman of the Department of Applied Chemistry, School of Chemical and Material Engineering, Jiangnan University, Wuxi, People's Republic of China. His research field is colloid and interface chemistry.